

and with ATP present (required for sarcolemmal ion gradients (high values). Then ionic substitution can large movement and VDCR as above. depolarization-induced Ca release in e (preventing T-tubule polarization, 1986). This argument also holds for R junctions. Second, as described at logical monovalent ions is very high SR and cytoplasm (Somlyo *et al.*, makes it likely that  $E_m = 0$  across the direct SR depolarization-induced SR T-tubules, but exhibit CICR). Thus, ble.

e extensively used the mechanically with sealed off T-tubules) to directly nditions can be readily manipulated. CR works by removing a tonic Mg-1 Fig 102 looks more like that for es skeletal, but not cardiac RyR. Mg larization would allow ambient  $[Ca]_i$  id Mg-dependent RyR inhibition.

Compelling evidence for VDCR. The RyR), these proteins are physically erway to understand this interaction sical and theoretical aspects. CICR Ca released by VDCR. Thus, while boost the initial rate of release.

that VDCR is not functional. 1) The t charge movement (Fig 106). 2) Ca uscle (Figs 105A & see below), 3) does not appear to modify Ca-induced e from cardiac corbular and extended l Ca release from corbular SR occurs ganization and interaction apparent in rt. Nevertheless, several groups have his possibility will be addressed (pg e in cardiac E-C coupling.

rom a phylogenetic standpoint. Most very similar to mammalian cardiac perspective is that CICR is very old

phylogenetically and has, in general, served well as an adaptive mechanism in heart (where speed of contraction is not of paramount importance). Thus, there may be weak physical interaction (direct or indirect) between cardiac DHPR and RyR, but these function mainly to keep sarcolemmal Ca channels in the neighborhood of clusters of RyRs. In fast-twitch skeletal muscle there is considerable adaptive advantage (survival) to high speeds of contraction. The vertebrate skeletal DHPR and RyR1 may have evolved additional points of interaction which are both more robust and also able to transmit the crucial E-C coupling signal very rapidly using the voltage sensor signal, without the need for Ca influx. In this context  $I_{Ca}$  in vertebrate skeletal muscle is essentially vestigial (for E-C coupling) and consequently the Ca channel function deteriorates with further evolution. This is consistent with the very slow activation of  $I_{Ca}$  (vs. charge movement or cardiac  $I_{Ca}$ ) in vertebrate skeletal muscle. These are just musings, of course.

## Ca-INDUCED Ca-RELEASE (CICR)

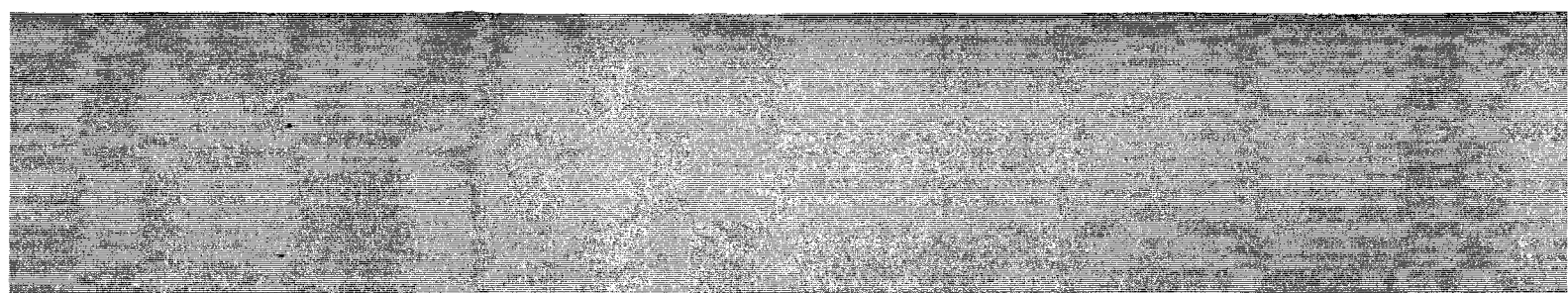
### *Ca-Induced Ca-Release in Skeletal Muscle*

CICR was first described in skinned skeletal muscle fibers (Endo *et al.*, 1970; Ford & Podolsky, 1970). While CICR exists in both cardiac and skeletal muscle (Chapter 7), the major question is whether it occurs physiologically and how it interacts with other possible mechanisms. Endo (1975a, 1977) argued that CICR was only demonstrable in skeletal muscle fibers at unphysiologically low  $[Mg]$ , required heavy SR Ca loading and very high trigger  $[Ca]$  (e.g. 100  $\mu M$  Ca with 0.9 mM Mg, or 10  $\mu M$  Ca with 50  $\mu M$  Mg). Fabiato (1984, 1985g) however, demonstrated CICR in skeletal muscle with the SR loaded at 100 nM Ca and  $\sim 3$  mV free  $[Mg]$ , triggered by a rapid  $[Ca]$  increase to 200-600 nM. The preceding section described how CICR and VDCR may coexist and function together in vertebrate skeletal muscle.

### *Ca-Induced Ca-Release in Mechanically Skinned Cardiac Muscle.*

Fabiato & Fabiato extensively characterized CICR in an elegant and formidable series of studies in mechanically skinned single cardiac myocytes (Fabiato & Fabiato, 1973, 1975a,b, 1978a,b, 1979; Fabiato 1981a, 1983, 1985a-c). In a culminating experimental series, Fabiato (1985a-c) used mechanically skinned canine Purkinje fibers because they lack T-tubules (which could reseal and complicate interpretations). The solutions included 5  $\mu M$  calmodulin (which slightly increased Ca release) and  $\sim 3$  mM free Mg. The largest CICR was seen in 1-3 mM Mg although the threshold  $[Ca]$  for CICR is higher than at lower  $[Mg]$  (Fabiato, 1983). Ca entry via  $I_{Ca}$  was simulated by very rapid Ca application, which induced SR Ca release. Solutions of various  $[Ca]$  at various rates could be applied as fast as  $\sim 1$  msec to these skinned cells and SR Ca release was measured using aequorin luminescence and force. Since CICR implies positive feedback, one might expect that Ca release would proceed to completion (as released Ca would cause more and more Ca release). However, a remarkable feature of CICR is that the amount of Ca released is graded with the amount of trigger Ca (Fabiato, 1983, 1985b). Indeed, at higher  $[Ca]$  CICR could be inhibited or inactivated (see below).

Figure 112A illustrates Fabiato's approach and shows inactivation of CICR at high  $[Ca]$ . In control contractions (C) the 100 nM Ca solution used to load the SR is withdrawn and 250 nM Ca solution applied briefly to activate SR Ca release (note that this  $[Ca]$  was insufficient to directly activate contraction; Fig 21A). In the third contraction (test) a higher  $[Ca]$  (10  $\mu M$ ) is



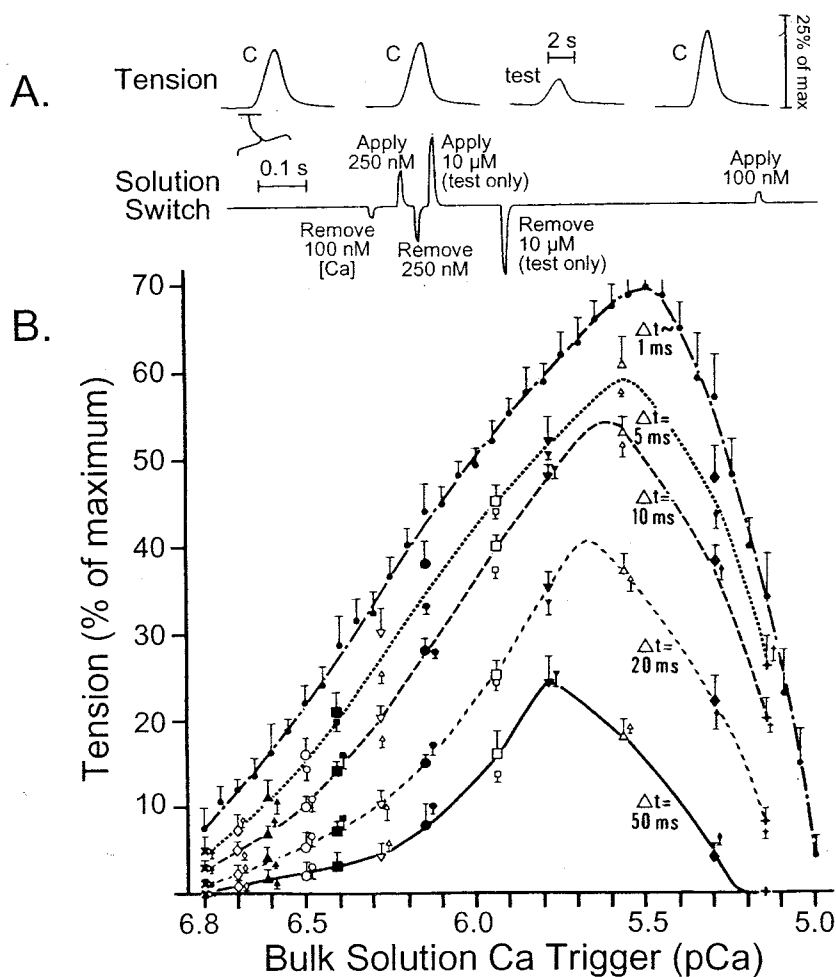


**Figure 112.** Fabiato's CICR in mechanically skinned canine cardiac Purkinje fiber. **A.** Tension recorded in response to rapid application and removal of experimental solutions of indicated [Ca] (lower trace is expanded time scale, as indicated by bar). In 100 nM [Ca] buffer the SR accumulates Ca. Removal of that solution and application of 250 nM Ca solution for 30 msec induces SR Ca release, peak [Ca] of 1.7  $\mu$ M and contraction (control traces, C). For the test contraction only, [Ca] was raised to 10  $\mu$ M for ~150 msec immediately after initiation of Ca release by 250 nM Ca. This extra elevation of [Ca] led to a smaller contraction and peak [Ca] (1.2  $\mu$ M), indicating Ca-dependent inactivation of SR Ca release. **B.** Relationship between trigger [Ca] for SR Ca release (as  $pCa = -\log [Ca]$ ) and the contraction amplitude resulting from CICR. Experiments were done like the controls in A, except trigger Ca was varied and the time taken to reach the trigger [Ca] was varied from 1 to 50 msec. Ca release depended on both trigger [Ca] and the rate of [Ca] change around the SR (modified from Fabiato, 1985b, with permission).

applied (for ~150 ms) right after the 30 ms pulse of 250 nM Ca. This higher [Ca] results in a smaller contraction and  $\Delta[Ca]_i$ . This indicates that the higher [Ca] inactivates the usual CICR.

Figure 112B shows the trigger [Ca] dependence of the tension transient produced by CICR (Fabiato, 1985b). Data are shown for several different durations taken to reach the indicated trigger [Ca]. It can be appreciated that the Ca released depends on both the trigger [Ca] and the time taken to reach that [Ca]. At high (or supra-optimal) trigger [Ca], the SR Ca release



rat skeletal muscle fiber. A. Tension recorded of indicated  $[Ca^{2+}]_i$  (lower trace is accumulated  $Ca^{2+}$ ). Removal of that  $Ca^{2+}$  release, peak  $[Ca^{2+}]_i$  of  $1.7 \mu M$  is raised to  $10 \mu M$  for  $\sim 150$  msec. Elevation of  $[Ca^{2+}]_i$  led to a smaller tension transient. B. Tension transient produced by various durations taken to reach the peak  $[Ca^{2+}]_i$  depends on both the trigger  $[Ca^{2+}]_i$  and the contraction amplitude. The time course depended on both trigger  $[Ca^{2+}]_i$  and the contraction amplitude (with permission).

This higher  $[Ca^{2+}]_i$  results in a smaller tension transient.

The tension transient produced by various durations taken to reach the peak  $[Ca^{2+}]_i$  depends on both the trigger  $[Ca^{2+}]_i$  and the contraction amplitude. The time course depended on both trigger  $[Ca^{2+}]_i$  and the contraction amplitude.

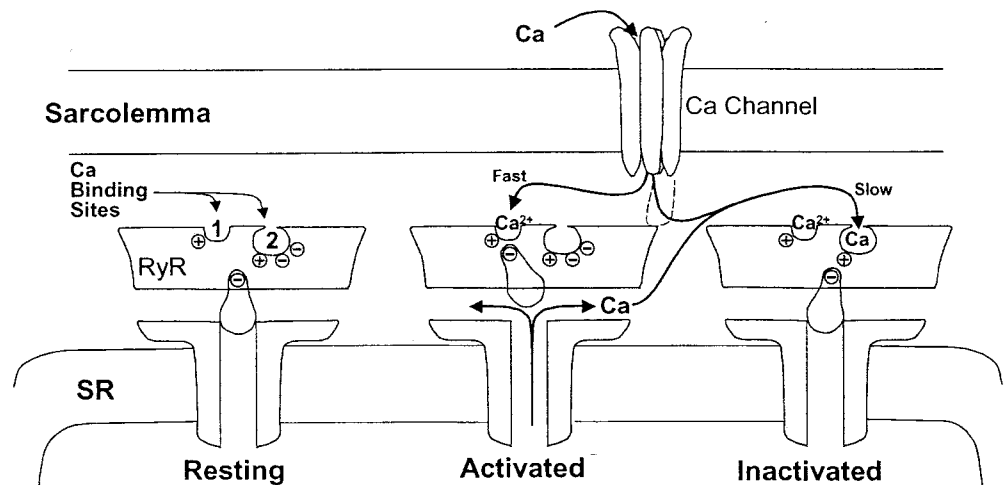


**Figure 113.** Diagram of CICR based on Fabiato's work. From the resting state (channel closed), Ca may bind rapidly to a relatively low affinity site (1), thereby activating the RyR. Ca may then bind more slowly to a second higher affinity site (2) moving the release channel to an inactivated state. As cytoplasmic  $[Ca^{2+}]_i$  decreases, Ca would be expected to dissociate from the lower affinity activating site first and then more slowly from the inactivating site to return the channel to the resting state.

was inhibited. CICR also exhibited a refractory period where a second Ca release could not be induced. This was not the case for caffeine-induced Ca-release. Fabiato (1985b) likened this to the inactivation (and recovery from inactivation) described for sarcolemmal Ca channels. He also showed that some steady state inactivation existed at  $63 \text{ nM } Ca$ , but that this inactivation could be removed by a few seconds at  $[Ca^{2+}]_i = 12 \text{ nM}$  (analogous to  $I_{Ca}$  inactivation and recovery).

On the basis of these findings Fabiato (1985b) proposed a model (Fig 113) where Ca binds to an activating site with a high *on rate* (but modest affinity) and also binds to a second inactivating site which has a higher affinity, but a slower association constant ( $\sim 0.7 \text{ sec}$  at  $[Ca^{2+}]_i = 63 \text{ nM}$ ). Thus, when  $[Ca^{2+}]_i$  increases rapidly the activation site is occupied and SR Ca release occurs. The inactivation site binds Ca more slowly to turn off Ca release. Rapid application of very high  $[Ca^{2+}]_i$  can still produce inactivation more directly since binding to the inactivation site is expected to be proportional to the product of *on rate* and  $[Ca^{2+}]_i$ . Thus, the very high  $[Ca^{2+}]_i$  can partially overcome the limitation of the slow *on rate*. This model provides a useful framework for understanding global behavior of E-C coupling at the cellular level in cardiac myocytes.

#### Ca-Induced Ca-Release: Support from Intact Cardiac Myocytes.

Figure 113 puts the sarcolemmal Ca channel close to the SR Ca release channel (RyR). Thus, Ca entry via  $I_{Ca}$  may have ready access to the activation (and inactivation sites) of the SR Ca release channel. The similar  $E_m$ -dependence of  $I_{Ca}$ , contraction and  $Ca^{2+}$  transient in cardiac myocytes (Fig 106A) are classic findings which are consistent with CICR in heart (London & Krueger, 1986; Cannell *et al.*, 1987; Beuckelmann & Wier, 1988; Callewaert *et al.*, 1988; duBell & Houser, 1989). Further support comes from the observation of  $I_{Ca}$  "tail transients" (Fig 114, Cannell *et al.*, 1987; Beuckelmann & Wier, 1988). These occur when a cell is first voltage clamped at positive  $E_m$  (e.g.  $+100 \text{ mV}$ ), where Ca channels are open, but no inward  $I_{Ca}$  is seen,

in the general range of 50-150  $\mu\text{mol/L}$  cytosol. For an SR Ca content of 100  $\mu\text{mol/L}$  cytosol we would require about 50% of this amount to be released in terms of the Ca requirements for activation of contraction (see Chapter 3). That conveniently matches estimates of fractional SR Ca release during the twitch (Bassani *et al.*, 1993b, 1995b).

### SR Ca RELEASE CHANNEL OR RYANODINE RECEPTOR

Isolation and molecular identification of the SR Ca-release channel was greatly accelerated by the recognition that the neutral plant alkaloid ryanodine is a selective and specific ligand for the channel (also called the ryanodine receptor, RyR). Ryanodine produces irreversible contracture of skeletal muscle, but progressive decline in cardiac muscle twitches (Jenden & Fairhurst, 1969; Hajdu & Leonard, 1961; Sutko & Willerson, 1980). Ryanodine opens the SR Ca release channel in both skeletal and cardiac muscle (see below). In cardiac muscle the Ca lost from the SR is extruded by Na/Ca exchange, thereby unloading the SR and cell of Ca, and depressing contractions. In skeletal muscle with much weaker Na/Ca exchange and higher SR Ca content, much of the SR Ca remains cytosolic, activating a contracture which consumes cellular ATP before the [Ca], declines (making contracture irreversible). Some useful RyR reviews are by Coronado *et al.* (1994), Meissner (1994), Sutko & Airey (1996), Xu *et al.*, (1998a), Zucchi & Ronca-Testoni (1997), Shoshan-Barmatz & Ashley (1998) and Sitsapesan & Williams (1998).

Ryanodine, at low concentrations (1-1000 nM), accelerates Ca loss from heavy SR vesicles, but at very high concentrations ( $>100 \mu\text{M}$ ) it slows Ca efflux (Fig 98D; Nayler *et al.*, 1970; Fairhurst & Hasselbach, 1970; Jones *et al.*, 1979; Jones & Cala, 1981; Fabiato, 1985d; Meissner, 1986a). Smith *et al.* (1985a, 1986) demonstrated that the Ca release from these heavy SR vesicles from skeletal muscle could be attributed to a high conductance Ca channel which they incorporated into lipid bilayers (i.e. the channel was similarly modulated by [Ca], ATP, ruthenium red and Mg). Rousseau *et al.* (1986, 1987) demonstrated similar channels in heart and also showed that ryanodine induced a long lived subconducting state of the SR Ca-release channel (Fig 98C). That is, ryanodine (at least up to 10  $\mu\text{M}$ ) appears to lock the Ca release channel into an open, but lower than normal conducting state. Williams and coworkers have shown that different ryanoids produce a different fraction of maximal conductance and also alter the dwell time in the open state (Tanna *et al.*, 1998, 2000). These studies have provided unique insights into the kinetics of ryanoid binding to the channel and also into conductance properties (see also review by Sutko *et al.*, 1997).

The ryanodine receptor (RyR) has a very high single channel conductance, especially when monovalent cations are the charge carrier (see Table 22). The RyR channel also has a relatively low Ca selectivity ( $P_{\text{Ca}}/P_{\text{K}} \sim 6$  vs. 3000 for the sarcolemmal Ca channel, Smith *et al.*, 1988 and see Table 17, pg 109). Indeed, even some relatively large organic monovalent cations can permeate, but the limiting pore diameter appears to be  $\sim 3.4 \text{ \AA}$  (Tinker & Williams, 1993). The length of the RyR pore (i.e. the narrow region where ions must shed their aqueous shell) has been estimated to be  $\sim 10 \text{ \AA}$ , by both streaming potential measurements and use of different length organic divalent cations (Tu *et al.*, 1994; Tinker & Williams, 1995).

nt of 100  $\mu\text{mol/L}$  cytosol we  
of the Ca requirements for  
es estimates of fractional SR

## RYANODINE RECEPTOR

lease channel was greatly  
ne is a selective and specific  
yR). Ryanodine produces  
in cardiac muscle twitches  
illerson, 1980). Ryanodine  
cle (see below). In cardiac  
ereby unloading the SR and  
uch weaker Na/Ca exchange  
tivating a contracture which  
e irreversible). Some useful  
& Airey (1996), Xu *et al.*,  
ey (1998) and Sitsapesan &

es Ca loss from heavy SR  
flux (Fig 98D; Nayler *et al.*,  
Cala, 1981; Fabiato, 1985d;  
Ca release from these heavy  
ductance Ca channel which  
y modulated by [Ca], ATP,  
similar channels in heart and  
state of the SR Ca-release  
ears to lock the Ca release  
illiams and coworkers have  
l conductance and also alter  
udies have provided unique  
into conductance properties

nel conductance, especially  
he RyR channel also has a  
al Ca channel, Smith *et al.*,  
organic monovalent cations  
(Tinker & Williams, 1993).  
hed their aqueous shell) has  
ments and use of different  
995).

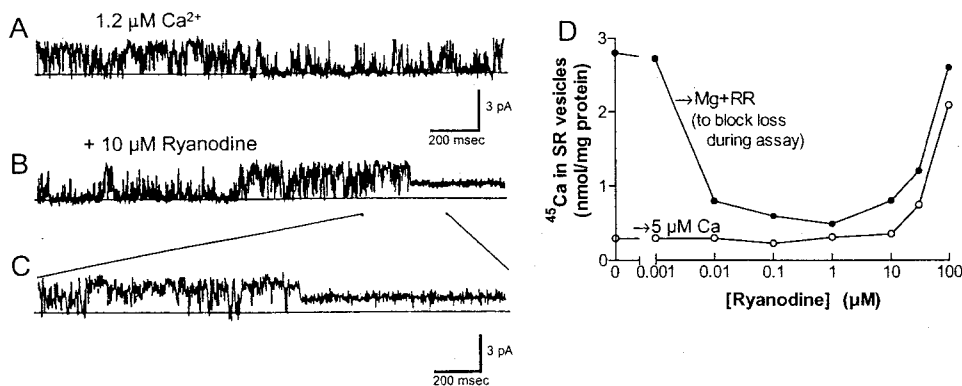


**Figure 98.** Ryanodine effects on cardiac SR Ca release channel. A-C. Recording from a single cardiac Ca release channel incorporated in a lipid bilayer. Currents are shown as upward deflections (from Rousseau *et al.*, 1987, with permission). The *cis* (cytoplasmic) side of the membrane contained 2.5  $\mu\text{M}$  free [Ca] and the *trans* side contained 50 mM Ba as the charge carrier (pH 7.4, 0 mV holding potential). Ryanodine was added 1 min before panel B was recorded. C. shows the transition from normal gating to a stable subconductance state on an expanded time scale. D. Dependence of  $^{45}\text{Ca}$  efflux from skeletal muscle SR vesicles on [ryanodine]. Vesicles were passively loaded with  $^{45}\text{Ca}$  (100  $\mu\text{M}$ ) and incubated for 45 min with ryanodine. They were then diluted into a Mg + ruthenium red (RR) medium, which blocks efflux (unless pretreated with 5 nM - 30  $\mu\text{M}$  ryanodine) or diluted into 5  $\mu\text{M}$  Ca medium which quickly emptied the vesicles (except at high [ryanodine]). Ryanodine causes SR Ca release at 5 nM to  $\sim 30 \mu\text{M}$ , but blocks release at 100  $\mu\text{M}$  (from Meissner, 1986a, with permission).

When Ca is used as the charge carrier, the conductance is lower than for monovalents and  $\geq 50 \text{ mM}$  Ca is typically used to obtain clear single channel data. Tinker *et al.* (1993) predicted that under more physiological conditions ( $[\text{Ca}]_{\text{SR}} = 2.4 \text{ mM}$ , 120 mM K and 0.5 mM Mg) the single channel Ca current would be 2 pA. This model prediction required extensive extrapolation. Mejia-Alvarez *et al.* (1999) made a concerted effort to approach physiological conditions with their single channel measurements and a unitary current of  $\sim 0.30 \text{ pA}$  can be inferred (at 2 mM  $[\text{Ca}]_{\text{SR}}$ , 150 mM [K], and 1 mM [Mg]). This single channel RyR current is only slightly larger than that of the sarcolemmal Ca channel ( $\sim 0.2 \text{ pA}$ ), but this is  $\sim 1$  million ions/sec or  $10^5$  times greater than turnover rate of the SR Ca-pump. The typical open time for a RyR is  $\sim 3 \text{ ms}$  (Tinker *et al.*, 1993).

### Molecular Identity and Structure of Ryanodine Receptors

Ryanodine was used as a specific ligand in the purification of the RyR from skeletal muscle (RyR1, Inui *et al.*, 1987a; Campbell *et al.*, 1987; Imagawa *et al.*, 1987b; Lai *et al.*, 1987, 1988a) and cardiac muscle (RyR2, Inui *et al.*, 1987b; Lai *et al.*, 1988b). Mammalian RyR1 has been cloned (MW = 565,223 Da; Takeshima *et al.*, 1989; Marks *et al.*, 1989; Zorzato *et al.*, 1990). The cardiac RyR2 has also been cloned (MW=564,711 Da; Otsu *et al.*, 1990; Nakai *et al.*, 1990) and a third isoform (RyR3) has also been cloned from brain (Hakamata *et al.*, 1992). These RyRs are products of 3 separate genes, but RyR1 & RyR2 are 66% identical and RyR3 is 67-70% identical to RyR1 and RyR2. Amphibian and avian skeletal muscle express  $\alpha$ ,  $\beta$  and cardiac isoforms and  $\alpha$  &  $\beta$  are similar to RyR1 & RyR3 (Sutko & Airey, 1996). Notably, with respect to E-C coupling issues to be discussed in the next chapter  $\alpha$  &  $\beta$  isoforms coexist in fast twitch frog skeletal muscle. Moreover, brain expresses both RyR2 and RyR1 in addition to

RyR3 (and the related intracellular Ca release channel, the IP<sub>3</sub> receptor) and there is a very small amount of RyR3 in mammalian skeletal muscle. Knocking out the RyR3 gene in mice does not prevent striated muscle function (Takeshima *et al.*, 1996). However, knocking out RyR1 in mice results in perinatal death (due to skeletal muscle failure, Takeshima *et al.*, 1994). Knockout of RyR2 is embryonically lethal, but this may not be due to defective cardiac E-C coupling at this developmental stage (Takeshima *et al.*, 1998).

**Table 22**  
**Cardiac Ryanodine Receptor Permeability and Conductance**

	$P_x/P_K$	Conductance (pS)*	Radius (Å)
K	1.00	723	1.33
Na	1.15	446	0.97
Cs	0.61	460	1.67
Li	0.99	215	0.68
Rb	0.87	621	1.47
Ca	6.5	135	0.99
Ba	5.8	202	1.34
Sr	6.7	166	1.12
Mg	5.9	89	0.66
ammonium	1.42	594	1.7
methylamine	0.67	286	1.9
ethylamine	0.51	105	2.2
dimethylamine	0.09	10	3.1
triethylamine	≤0.04	≤10	3.6

Relative permeability is based on reversal potential shifts in bionic conditions.  
\*Conductances in 210 mM permeant ion. Data are from Williams (1998).

The tetrameric nature of the ryanodine receptor *in vivo* implies a 2,260,000 Da structure. The protein appears to exist mainly as a homotetramer, based on its quatrefoil appearance (Saito *et al.*, 1988; Lai *et al.*, 1988a; Wagenknecht *et al.*, 1989), gel permeation chromatography (Inui *et al.*, 1987a) and stoichiometry of high affinity ryanodine binding (Lai *et al.*, 1988a, 1989). The large size of this homotetramer has helped to identify it ultrastructurally as the junctional foot process which spans the gap between the SR and sarcolemmal membranes at their junctions. Thus, it traverses the SR membrane providing a channel for SR Ca release and also extends toward the sarcolemmal membrane. This proximity is undoubtedly important in the process of triggering SR Ca release during E-C coupling (see Chapter 8).

Three-dimensional reconstructions of the RyR based on electron microscopic images have been continuously refined (Wagenknecht *et al.*, 1989; 1994, 1996; 1997; Sasmó *et al.*, 1999; Serysheva *et al.*, 1995, 1999). Figure 99 shows three different views of the RyR. Sites are also indicated where calmodulin and FK-506 binding proteins (FKBP) interact with the RyR (see pg 198). The complex is ~28 nm along each side and ~14 nm high above the SR membrane, which correspond to the width and length of the junctional "feet" observed ultrastructurally in electron micrographs of intact muscle (see Chapter 1). The RyR reconstructions are intriguing because some suggest a channel for Ca flux going through the center of the molecule from the SR lumen and possibly coming out the sides of the RyR into the junctional space (Fig 88 and

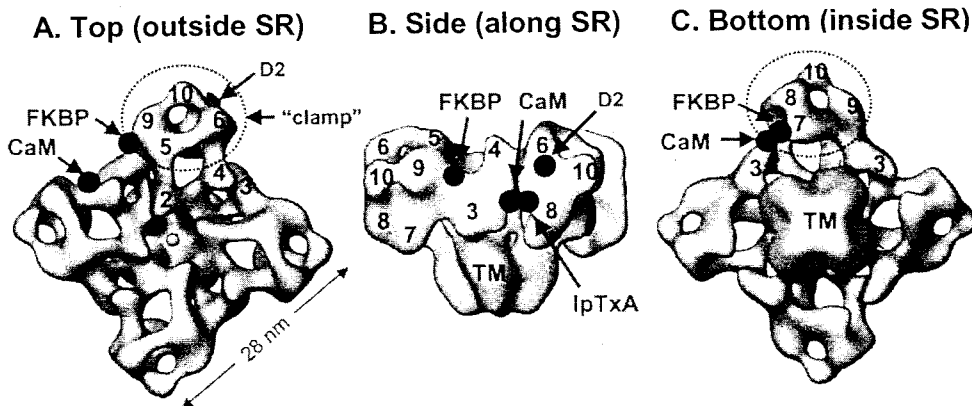


**Figure 99** Three-dimensional reconstruction of the skeletal muscle ryanodine receptor. Three views **A.** from top or T-tubule, **B.** from along the plane of the SR membrane and **C.** from within the SR lumen. Selected cytoplasmic domains are numbered. "clamp" (dashed circle) refers to domains 5-10 that form each corner of the cytoplasmic region; TM, transmembrane region; IpTxA, Imperatoxin A; CaM, calmodulin; D2, divergency region 2 (amino acids 1303-1406); FKBP, FK506-binding protein. Figure generously provided by T. Wagenknecht.

Serysheva *et al.*, 1999). In Fig 99 the FKBP site is ~9 nm away from the calmodulin site. The FKBP location may be relevant to functional observations which suggest that FKBP is important in coupling monomers within the tetrameric array as well as between tetramers (Brilliantes *et al.*, 1994; Kaftan *et al.*, 1996; Marx *et al.*, 1998a). There is also some initial information about which RyR1 sites might interact with the skeletal L-type Ca channel,  $\alpha_{1S}$  or imperatoxin A (Nakai *et al.*, 1998a; Sasmo & Wagenknecht, 1998; Grabner *et al.*, 1999).

The high affinity effects of ryanodine on SR vesicles coupled with observations from more intact preparations (e.g. Sutko *et al.*, 1985) led to the use of ryanodine as a specific ligand in binding studies with SR vesicles (Pessah *et al.*, 1985; Fleischer *et al.*, 1985; Alderson & Feher, 1987; Imagawa *et al.*, 1987b; Inui *et al.*, 1987a; Lattanzio *et al.*, 1987; Meissner & Henderson, 1987). The affinity of the receptor for ryanodine is dependent on [Ca] and the presence of nucleotides (e.g. ATP), but in the conditions typically used  $K_d$  values are 4-36 nM.

Figure 100 shows some key RyR domains. The number of suggested transmembrane spanning domains ranges from 4-12 (Takeshima *et al.*, 1989; Otsu *et al.*, 1990) with at least M1-M4 consistent with most data (Balshaw *et al.*, 1999). Results from the related IP<sub>3</sub> receptor are more compelling for 6 transmembrane spans (Michikawa *et al.*, 1994; Mignery *et al.*, 1989; Galvan *et al.*, 1999) making 4-6 seem plausible for RyR2 until clearer data are available. A human RyR1 mutation (I4898T) produces central core disease (Lynch *et al.*, 1999; see below) and site directed mutagenesis studies in this M3-M4 region (including GIG, as in Na/Ca exchanger & GYG in K channels) has identified this as the pore loop in RyR2 and RyR1 (Zhao *et al.*, 1999; Balshaw *et al.*, 1999; Gao *et al.*, 2000). This is analogous to the IP<sub>3</sub> receptor domain where the channel pore has been shown to reside (the 5<sup>th</sup>-6<sup>th</sup> transmembrane spans including an intervening GGVG sequence, Ramos-Franco *et al.*, 1999). Marx *et al.* (2000) demonstrated that the cardiac RyR is really a megacomplex including FKBP12.6, a PKA anchoring protein

tor) and there is a very small RyR3 gene in mice does not; knocking out RyR1 in mice *a et al.*, 1994). Knockout of cardiac E-C coupling at this

## Conductance

### Radius (Å)

1.33  
0.97  
1.67  
0.68  
1.47

0.99  
1.34  
1.12  
0.66

1.7  
1.9  
2.2  
3.1  
3.6

ionic conditions.  
ams (1998).

ies a 2,260,000 Da structure. quatrefoil appearance (Saito tion chromatography (Inui *et al.*, 1988a, 1989). The urally as the junctional foot embranes at their junctions. Ca release and also extends important in the process of

lectron microscopic images 1996; 1997; Sasmó *et al.*, views of the RyR. Sites are ) interact with the RyR (see h above the SR membrane, observed ultrastructurally in onstructions are intriguing er of the molecule from the nctional space (Fig 88 and

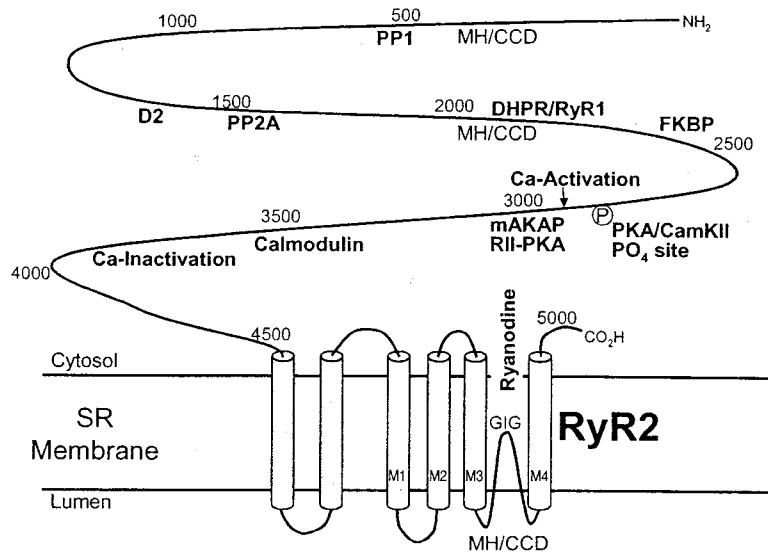


**Figure 100** Schematic of domains in cardiac ryanodine receptor sequence. The 4 transmembrane domains M1-M4 are according to Takeshima *et al.* (1989) and there may be 2 more. Approximate locations along the primary structure of several sites of either interaction (e.g. phosphatases 1 & 2A, PP1 & PP2A; mAKAP, kinase anchoring protein), a putative pore region (GIG), PKA/CaMKII phosphorylation site (P) and Ca effector sites. A few sites important in RyR1 are also shown, e.g. mutation sites associated with malignant hyperthermia or central core disease (MH/CCD) and sites where skeletal muscle DHPRs may interact (1635-2636 & 2659-3720, Nakai *et al.*, 1998a). Figure kindly supplied by A.R. Marks.

(mAKAP) and two phosphatases (PP1 & PP2A) in addition to interactions with calmodulin and junctin/triadin described above. These associated proteins will be discussed further below.

#### *Ca sparks: Fundamental Cellular SR Ca Release Events*

SR Ca release in the intact myocyte appears to occur via relatively stereotypical local events referred to as Ca sparks (Fig 101, sensed by fluorescent Ca indicators). These Ca sparks (first described by Cheng *et al.*, 1993) occur during rest (at very low frequency) in a stochastic manner, even in the absence of Ca influx. The normal twitch Ca transient in ventricular myocytes is also likely composed of a temporal and spatial summation of thousands of Ca spark events which are synchronized by the AP and  $I_{Ca}$  via Ca-induced Ca-release (Cannell *et al.*, 1994, 1995; López-López *et al.*, 1994, 1995).

Figure 101A shows two spontaneous Ca sparks in a resting mouse ventricular myocyte during acquisition of a 2-dimensional image. To enhance temporal resolution it is customary to use the line scan mode of the confocal microscope. The whole length of this cell was scanned every 2 ms along a line avoiding nuclei. Figure 101B shows a line scan image with a single prominent Ca spark, where distance along the cell length is shown in the vertical dimension and time along the horizontal dimension. Figure 101C shows the  $[Ca]_i$  in the narrow region of the cell where the Ca spark occurs. The surface plot (Fig 101D) shows the time and spatial dependence of local  $[Ca]_i$  during this single Ca spark. Ca sparks originate at the T-tubule (Cheng *et al.*,

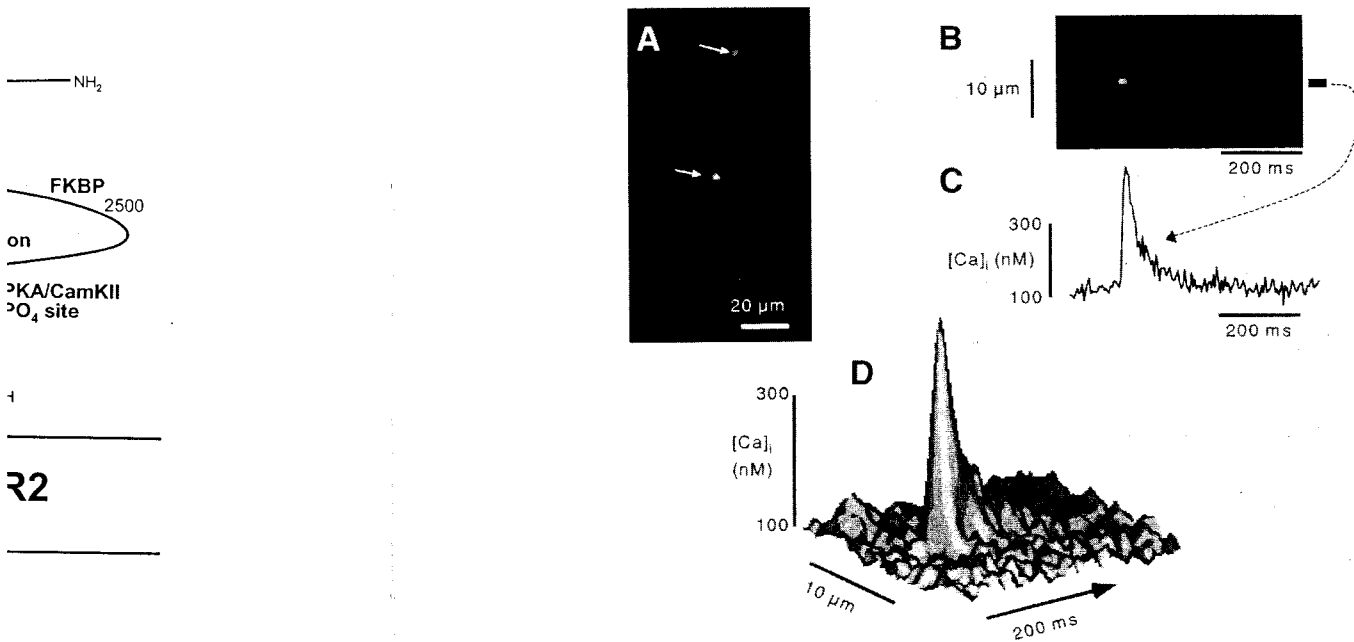


**Figure 101** Ca sparks in isolated mouse ventricular myocyte. **A.** Two dimensional laser scanning confocal fluorescence image of myocyte loaded with the Ca-sensitive indicator fluo-3, exhibiting two Ca sparks (arrows). **B.** Line scan image along the long axis of the myocyte (only part is shown). Scans were repeated every 4 ms and stacked from left to right. Distance along the cell is in the vertical direction. **C.** Line graph of [Ca]<sub>i</sub> at the spot indicated by the bar in B (~1 μm). **D.** Surface plot of [Ca]<sub>i</sub> during a Ca spark, indicating the temporal and spatial spread of Ca (figure kindly supplied by L.A. Blatter).

ence. The 4 transmembrane  
2 more. Approximate locations  
hatases 1 & 2A, PP1 & PP2A;  
FKBP 2500  
on  
PKA/CamKII  
O<sub>4</sub> site  
1  
R2

ctions with calmodulin and  
cussed further below.

relatively stereotypical local  
dicators). These Ca sparks  
v frequency) in a stochastic  
Ca transient in ventricular  
on of thousands of Ca spark  
Ca-release (Cannell *et al.*,

mouse ventricular myocyte  
resolution it is customary to  
th of this cell was scanned  
e scan image with a single  
the vertical dimension and  
in the narrow region of the  
the time and spatial depen-  
the T-tubule (Cheng *et al.*,

1996; Parker *et al.*, 1996) and typically reach a peak [Ca]<sub>i</sub> of 200-300 nM in ~10 ms, have a spatial spread of ~2 μm (full width half-maximum) and [Ca]<sub>i</sub> declines with a time constant of ~25 ms. The decline of local [Ca]<sub>i</sub> during the Ca spark is largely due to Ca diffusing away from the site of release. However, we showed that when the SR Ca-ATPase was blocked in rat (by thapsigargin) [Ca]<sub>i</sub> decline during a spark was slowed by 26% (and spatial spread also broadened, Gómez *et al.*, 1996). This represents [Ca]<sub>i</sub> decline attributable to diffusion away from the source (i.e. both SR Ca-ATPase and Na/Ca exchange were blocked). Conversely, when we stimulated SR Ca-ATPase by PKA activation, local [Ca]<sub>i</sub> decline was accelerated by 33% (or 50% compared to diffusion alone). Thus Ca transport rate can effect spatial and temporal spread of Ca sparks and influence their activation of neighboring RyRs via Ca-induced Ca-release.

#### Quantitative Aspects of SR Ca release Flux

Cheng *et al.* (1993) estimated the Ca flux associated with a single Ca spark as ~2×10<sup>-19</sup> mol (or 40 fC) and proposed that this might be due to a single RyR channel event (4 pA×10 ms). A more realistic single RyR channel flux is ≤ 2 fC (0.4 pA × 4 ms, see pg 187). This would be consistent with a cluster of ~20 release channels contributing to a single Ca spark. This is in the range of the clusters of 50-200 feet/RyRs at dyadic junctions in heart (Franzini-Armstrong *et al.*, 1999; see pg 14). Attempts to measure the number of RyRs involved in a Ca spark have been challenging (e.g. measuring smaller events or titrating some of the RyRs with blockers), but have given values in the range of 6-20 (Parker *et al.*, 1996; Lipp & Niggli, 1996; Blatter *et al.*, 1997;

Bridge *et al.*, 1999; Lukyanenko *et al.*, 2000). It is clear now that a Ca spark is due to a cluster of RyRs working as a functional unit (discussed further in Chapter 8).

To explain a resting SR Ca leak rate of  $0.3 \mu\text{mol/L}$  cytosol (Bassani and Bers, 1995) requires about 50 Ca sparks/sec in the cell (or  $\sim 2$  sparks/pL/sec). This is typical of the resting Ca spark frequency observed in ventricular myocytes (Cheng *et al.*, 1993; Satoh *et al.*, 1997) and is consistent with virtually all of the resting leak of Ca from the SR being attributed to these occasional Ca sparks.

How many RyRs are there in a typical ventricular myocyte? Bers & Stiffel (1993) measured 504, 656, 833 and 1,144 fmol/mg protein RyR in ventricular myocytes from rabbit, guinea-pig, rat and ferret, respectively. This corresponds to  $0.08$ - $0.19 \mu\text{mol/L}$  cytosol RyR or 1.5-3.5 million RyR in a 30 pL myocyte (500 times fewer than SR Ca-pumps). For a resting rate of 50 Ca sparks/sec, only 1,000 RyR need to open each second (or 0.02% of the cell's RyRs). To attain a peak SR Ca release flux of 3 mM/s estimated by Wier *et al.* (1994), would require simultaneous activation of about 40,000 RyR (only  $\sim 2\%$  of the cell's complement of RyRs). Furthermore, a total SR Ca release flux of  $50 \mu\text{mol/L}$  cytosol would also require only  $\sim 7,500$  Ca sparks (based on 40 fC/spark) or  $\sim 5\%$  of the cellular RyRs (based on 2 fC/RyR). Thus, normal twitch activation only requires a small fraction of available RyRs to function at any given twitch.

It is of interest to note here that opening of a similarly modest fraction of L-type Ca channels (2-3%) is required to produce the measured whole cell  $I_{Ca}$  (pg 114; Lew *et al.*, 1991). For example, there may be  $\sim 250,000$  dihydropyridine receptors in a 30 pL rat ventricular myocyte, but only  $\sim 5,000$  Ca channels need to open (with a single channel current of 0.2 pA to produce a peak whole cell current of 1 nA).

#### *Regulation of SR Ca Release*

The most direct and compelling data about SR Ca release channel regulation come from measurements of single RyR currents in lipid bilayers. Those studies are challenging and still have the caveats that a) the channels are not in their native physiological environment and b) the behavior of one channel is assumed to be representative of the population of RyRs. For many aspects there is also corroborative evidence from measurements of Ca efflux from heavy SR vesicles, ryanodine binding and cellular experiments. Cellular experiments are necessarily more complex to interpret, but have the advantage of being in a more physiological context. Measurement of  $^3\text{H}$ -ryanodine binding is simple, but useful because ryanodine binds strongly to the open RyR channel, thus higher ryanodine binding (at sub- $B_{\text{max}}$  conditions) can correlate with greater open probability (Xu *et al.*, 1998a), although the inference is indirect. Table 23 shows effects of several factors on RyR gating (see also reviews by Palade, 1987a,b,c; Coronado *et al.*, 1994; Zucchi & Ronca-Testoni, 1997; Shoshan-Barmatz & Ashley, 1998; Xu *et al.*, 1998a).

Figure 102 shows that Ca activation of the cardiac RyR begins at sub-micromolar  $[\text{Ca}]$ , reaches a broad maximum (at very high  $P_o$ ) near  $100 \mu\text{M}$  Ca and decreases at very high  $[\text{Ca}]$  (5-10 mM, Rousseau & Meissner, 1989; Xu *et al.*, 1998a). The skeletal muscle RyR is less strongly activated by Ca alone, requiring more Ca for activation, reaching a lower peak  $P_o$  (near  $10 \mu\text{M}$  Ca) and almost completely inactivating by 1 mM Ca. ATP (and other adenine nucleotides) activate cardiac RyR channels, but only if  $[\text{Ca}]$  is high enough to partially activate the channel